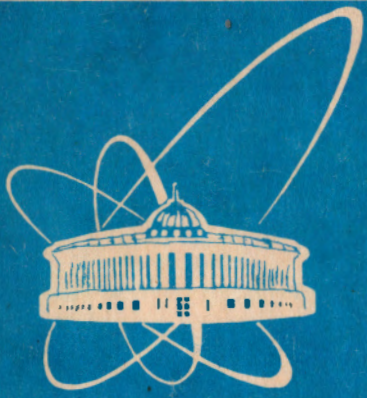

сообщения
объединенного
института
ядерных
исследований
дубна

E9-94-369

V.Anguelov[1], D.Dinev[1], I.Dmitriev[2],
V.Mikhailov, S.Tzenov[1]

CHARGE EXCHANGE INJECTION OF HEAVY IONS IN SYNCHROTRONS*

[1]Institute for Nuclear Research and Nuclear Energy, Sofia, Bulgaria
[2]Institute for Nuclear Physics of Moscow State University
*Work supported by the Bulgarian National Science Foundation under Contract No. F-309

1994

1. INTRODUCTION

This paper concerns the problems of charge exchange injection of heavy ions into synchrotrons. Charge exchange injection now is now the preferred injection method for proton machines due to its relative simplicity and a very high intensity of stored beams.[1,2] Recently this injection method has been successfully applied for light ion storage in the CELSIUS [3] and COSY [4] cooler rings. In this pape work we try to analyse the possibility for the charge exchange injection method to be applicable to heavy ions. A detailed analysis of the beam-stripper interaction processes and their reflection on beam dynamics is carried out. The deduced theoretical relations are applied to the the NUCLOTRON booster[5] being under design at Laboratory of High Energies of JINR. Dubna.

2. BOOSTER SYNCHROTRON FOR THE SUPERCONDUCTING HEAVY ION SYNCHROTRON NUCLOTRON

A booster synchrotron[5] is being designed for the Dubna super conducting heavy ion synchrotron NUCLOTRON [6]. The booster will be a fast synchrotron with a circumference of 50 m and a repetition frequency of 1 Hz. It will be able to accelerate ions up to 200 MeV/nucleon and protons up to 650 Mev. The booster will give the NUCLOTRON new capabilities for experiments at middle and high energies by improving the quality of its beams. The circumference of the booster will be 1/5 of the NUCLOTRON one so that 5 successive pulses can be injected into the NUCLOTRON. Thus, the total injection time will be about 4 sec, and the beam intensity will be improved by one order of magnitude at least. Letting the booster beam pass through a stripping foil one will be able to increase the ion charge and thus to increase the final energy in the NUCLOTRON.

An electron cooling system is being planned for the booster. It will reduce the beam emittance and momentum spread up to one

order of magnitude. The booster can be used in an autonomous regime as well.

The booster magnetic structure consists of 6 periods, each of them comprising two bending magnets and a quadruplet of quadrupole lenses.

This paper deals with the injection schemes of heavy ions in the booster synchrotron. Several injection methods are considered:

i) multiturn injection with filling the horizontal acceptance;

ii) high frequency ion stacking.

iii) multiturn injection with filling the four dimensional transverse phase space using the linear coupling resonance $Q_x = Q_y$.

iv) charge exchange injection

It is the charge exchange injection that will be particularly considered in the present paper.

Main booster parameters are listed in Table 1 below.

Table 1

Booster Synchrotron Parameters

Circumference			50.52 m
Energy	injection	ions $\frac{Z}{A}=0.5$	5 MeV/n
		protons	20 MeV
	maximum	ions $\frac{Z}{A}=0.5$	200 MeV/n
		protons	650 MeV
Beam rigidity	at injection		0.647 Tm
	maximum		4.3 Tm
Betatron tune	$Q_x = Q_y =$		2.25
Emittance	at injection		40π mm.mrad
	at the end of the cycle		40π mm.mrad
Acceptance	$A_x = A_y =$		260π mm.mrad
Momentum spread			$\pm 2.10^{-3}$
Number of periods			6
Number of dipoles			12
Number of quadrupoles			24

3. CHARGE-EXCHANGE INJECTION IN SYNCHROTRONS

The principle of charge exchange injection consists in letting a injected beam pass through a thin internal foil. /1/ Having passed the foil ions change their charge while energy is practically unaltered and beam rigidity $B\rho$ jumps to a new value according to the well-known relation:

$$B\rho = \frac{A}{300Z} \sqrt{T_n^2 + 2E_{0n}T_n} \qquad (3.1)$$

where $B\rho$ is in Tm: the kinetic energy T_n per nucleon is in MeV and the rest of energy per nucleon E_{0n} is also in Mev. This provides a spatial separation for the trajectories of the injected and circulating beams.

The charge exchange process cannot be described by the Hamiltonian system. That is why the Liouville theorem for phase space density conservation does not work. This allows us to inject ions many times into one and the same area in the phase space thus increasing the intensity of the stored beam (non-Liouville stacking).

4. INJECTION BUMP

During the stripping injection, a local orbit bump should be produced for the beam to pass through the stripping foil. For the booster case a height of 70 mm has been chosen for this bump. The booster bump will be produced by means of four bump magnets situated between the ring dipole magnets.

Let us consider the kicks in the bump magnets necessary for the local closed orbit bump to be produced. Here we will analyze the general case of arbitrary phase distances between the elements as given in /6/.

A. Systems with Three Bumpers

A scheme of three bumpers scheme is depicted in Fig.1.

The kicks ε_1, ε_2 and ε_3 which produce a closed orbit bump with deviation X_t in the stripping target are the solutions of the following system of three equations:

$$\sin \mu_{13} \sqrt{\beta_1}\, \varepsilon_1 + \sin \mu_{23} \sqrt{\beta_2}\, \varepsilon_2 = 0$$
$$\cos \mu_{13} \sqrt{\beta_1}\, \varepsilon_1 + \cos \mu_{23} \sqrt{\beta_2}\, \varepsilon_2 + \sqrt{\beta_3}\, \varepsilon_3 = 0 \qquad (4.1)$$
$$\sin \mu_{t3} \sqrt{\beta_3}\, \varepsilon_3 = \frac{x_t}{\sqrt{\beta_t}}$$

where $\varepsilon_1 = \frac{B_1 l_1}{B\rho}$ is the kick in the first bumper and μ_{12} is the phase advance between BM_1 and BM_2 $\left(\mu_{12} = \int_1^2 \frac{d\alpha}{\beta(\alpha)} \right)$.

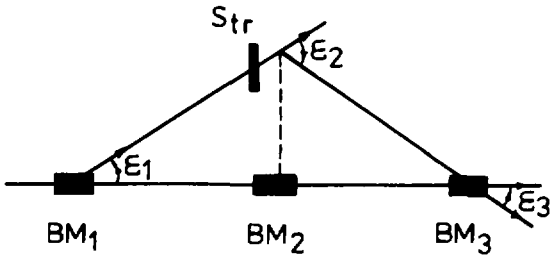

Figure 1. Injection system with three bump magnets.

B. System with Four Bumpers

Using a system with four bumpers an additional constraint of having a zero slope at the stripping target can be set - Fig. 2. Two cases can be distinguished.

In the first case a drift space is situated between the second and the third bump magnets. Using the Twiss form of transfer matrix, we obtain for the kick in the first bumper:

$$\varepsilon_1 = \frac{x_t}{m_{12}^1} = \frac{x_t}{\sqrt{\beta_{c1}\beta_{c2}}\, \sin \mu_{12}} \qquad (4.2)$$

where we have denoted by M^1 the transfer matrix from C_1 to C_2. and by M^2 the transfer matrix from C_2 to the stripping target.

The kick in the second bumper should counteract the trajectory slope X':

$$\varepsilon_2 = - X'_2 = -m^1_{22}\,\varepsilon_1 - - \frac{X_t}{\beta_{c2}} (\operatorname{ctg} \mu_{12} - \alpha_2) \qquad (4.3)$$

Finally from a symmetry:

$$\varepsilon_3 = - - \frac{X_t}{\beta_{c3}} (\operatorname{ctg} \mu_{34} - \alpha_3)$$

$$\varepsilon_4 = \frac{X_t}{\sqrt{\beta_{c3}\beta_{c4}}\,\sin \mu_{34}} \qquad (4.4)$$

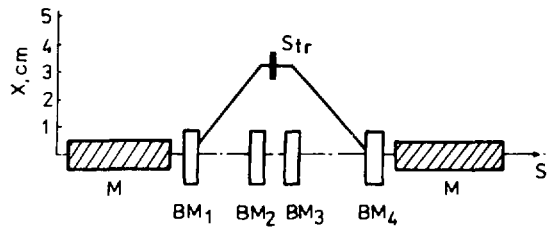

Figure 2. Injection system with four bump magnets.

In the second case when no drift space but some elements (quadrupoles, for instance) lie between the second and the third bumper, it is still possible to obtain a zero slope in the stripping target although the trajectory is more complicated.

For the strengths of the first two bump magnets one can deduce in this case:

$$X_t = \sqrt{\beta_{c1}\beta_t}\ \frac{\sin \mu_{12}}{(\cos \mu_{2t} - \alpha_t \sin \mu_{2t})}\ \varepsilon_1$$

$$\varepsilon_2 = -\sqrt{\frac{\beta_{c1}}{\beta_{c2}}}\ \frac{(\cos \mu_{1t} - \alpha_t \sin \mu_{1t})}{(\cos \mu_{2t} - \alpha_t \sin \mu_{2t})}\ \varepsilon_1 \qquad (4.5)$$

And from a symmetry:

$$X_t = \sqrt{\beta_t\beta_{c4}}\ \frac{\sin \mu_{34}}{(\cos \mu_{t3} - \alpha_t \sin \mu_{t3})}\ \varepsilon_4$$

$$\varepsilon_3 = -\sqrt{\frac{\beta_{c4}}{\beta_{c3}}}\ \frac{(\cos \mu_{t4} - \alpha_t \sin \mu_{t4})}{(\cos \mu_{t3} - \alpha_t \sin \mu_{t3})}\ \varepsilon_4 \qquad (4.6)$$

Necessary strengths of the bump magnets in the NUCLOTRN booster were calculated according to relations (4.2-4.4) and a posteriori improved by particle tracking using the computer code MAD /7/. The tracking results are shown in Table 2. The required kicks are less than 0.1 rad.

Table 2

No	$\mu*2\pi$	β.m	x.mm
BM_1	2.183	4.763	0.0
BM_2	2.210	4.514	71.536
BM_3	0.011	4.514	71.536
BM_4	0.038	4.763	0.0

5. EQUILIBRIUM CHARGE STATE DISTRIBUTION AND EQUILIBRIUM THICKNESS OF THE STRIPPING FOIL

As the beam ions travel through the matter a relative content of ions in different charge states changes. The process is described by the following set of linear differential equations:

$$\frac{d\Phi_k}{dt} = \sum_j \Phi_j \sigma_{jk} \qquad (5.1)$$

where Φ_i is the percentage of the ions in the j-th charge state in the beam: σ_{jk} is the cross-section for the transition j→k; t is the foil thickness in at/cm^2.

The charge state distribution reaches equilibrium for thick enough foils [8,9]. This equilibrium distribution undependent of the initial distribution in the beam is determined only by the relations between different charge exchange cross-sections σ_{jk} and the ion velocity. The beam attains charge state distribution equilibrium earlier than a visible particle delay in the foil material is reached. The equilibrium distribution is the solution of the linear system:

$$\sum_j \Phi_j \sigma_{jk} = 0 \qquad (5.2)$$

So in order to calculate for the equilibrium distribution and the equilibrium thickness to be calculated one needs the exact values of electron loss and capture cross-sections σ_{jk}. First theoretical papers on the cross-sections in ion-atom collisions have been carried out by N.Bohr. He found for the electron loss[10]:

$$\sigma_e \approx 4\pi a_0^2 \frac{Z_t^2 + Z_t}{q^2} \left(\frac{\beta_i}{\alpha}\right)^{-2} \qquad (5.3)$$

where α=1/137 is the fine structure constant and a_0 is the Bohr's radius, and for electron capture (together with Lindhard) [11] we have:

$$\sigma_c = \pi a_0^2 Z_t^{1/3} q^2 \left(\frac{\beta_i}{\alpha}\right)^{-3} \qquad (5.4)$$

Unfortunately, the experiments have shown that the above formulae work well only over a quite narrow range of parameters. A lot of semi-empirical formulae for electron loss and capture cross-sections have been put forward [12-14].

For electron capture the experiments show that:

$$\sigma_c \sim Z_{pr}^{\alpha_1} v^{\alpha_2} Z_t^{\alpha_3} \qquad (5.5)$$

where

$$\alpha_1 = 4 \div 5 \; ; \; \alpha_2 = -(2 \div 5) \; ; \; \alpha_3 = 0.15 \div 0.4$$

The electron loss cross-section σ_e increases with target atomic number Z_t and decreases with projectile atomic number Z_{pr} ($\sigma_e \sim Z_{pr}^{\alpha}$, $\alpha = -(1 \div 3)$) and depends strongly on the ion velocity. On the other hand, the experiments show that the cross-sections for losses of more than one electron are not negligible. In connectionwith that there were proposed a semiempirical method[14a] for calculations the cross sections for the loss of one and sveral electrons by fast multielectron ions. Using this methpod, which is based on the results of an analysis of experimental data and theoretical calculations the cross sections (m=1-5) have been obtained tor the fast ions of iodine and uranium in nitrogen.

The problem is even more complicated as the case of solid foils strongly differs from that of rare gases. While inrare gases the time between the successive ion-atom collisions is long enough for excited atoms to return to their basic state in solid foils this time is short and the atom state remains almost unchangeable. This means that all the cross-sections should be averaged over the excited states. For this reason the electron loss cross-sections in solids are larger than in gases and the electron capture cross-sections are smaller. As a result the equilibrium thicknesses in solid foils are larger (p to ten times) than those in gases[15].

The accelerator experiments [16.17] show that for heavy ions with energies from 3.8 to 10.6 MeV/nucleon the equilibrium thickness of carbon foils lies between 250 to 350 $\mu g/cm^2$.

6. EQUILIBRIUM CHARGE STATE DISTRIBUTIONS BEHIND THE STRIPPING FOIL

The equilibrium charge state distributions of heavy ion beams on traversing the stripping foil are presented by a Gaussian /18/ although the Gaussian describes continuous random variables while the ion charge states q are discrete ones.

$$\Phi_q = \frac{1}{\sigma\sqrt{2\pi}} e^{-\frac{(q-\bar{q})}{2\sigma^2}} \qquad (6.1)$$

Formula (6.1) is valid if the average charge state $\bar{q}$ is not too close to Z_{pr}.

Several empirical formulae have been proposed for the average charge state $\bar{q}$. It is assumed to use the reduced velocity X as an independent variable in all of these formulae:

$$X = \frac{V}{V' Z_{pr}^{0.45}} \quad , \quad V' = 3.6\ 10^8 \text{ cm/s} \qquad (6.2)$$

Nikolaev - Dmitriev's formula /19/:

$$\frac{\bar{q}}{Z_{pr}} = (1 + X^{-\frac{1}{0.6}})^{-0.6} \qquad (6.3)$$

To - Droin's formula /20/:

$$\frac{\bar{q}}{Z_{pr}} = 1 - e^{-X} \qquad (6.4)$$

Shima's formulae /21/:

$$\frac{\bar{q}}{Z_{pr}} (Z_t = 6) = 1 - \exp(-1.25\,X + 0.32\,X^2 - 0.11\,X^3) \qquad (6.5)$$

$$\frac{\bar{q}}{Z_{pr}} (Z_t \neq 6) = \frac{\bar{q}}{Z_{pr}} (Z_t = 6) [1 + g(Z_t)] \qquad (6.6)$$

where

$$g(Z_t) = - 0.0019 (Z_t - 6) \sqrt{X} + 10^{-5} (Z_t - 6)^2 X \qquad (6.7)$$

Heckman - Betz's formula /22-24/:

$$\frac{\bar{q}}{Z} = 1 - C \exp\left[- \frac{V}{V_0 Z_{pr}^{\gamma}} \right] \qquad (6.8)$$

where C and γ are constants depending on Z_{pr} in the intervals :
$C \in (1.07 \div 1.25) : \gamma \in (0.57 \div 0.65)$
and $v_0/c = 137$.
Baron - Ricaud's formula /16/:

$$\frac{\bar{q}}{Z} = 1 - C \exp (- \frac{83.275\beta}{Z^{0.447}}) \qquad (6.9)$$

where $C = \begin{cases} 1, \text{ for } T_{pr} > 1 \text{ MeV/n.} \\ 0.9 + 0.0769\ T_{pr}, \text{ for } T_{pr} < 1 \text{ MeV/n} \end{cases}$

Formulae (6.1-6.5) have been deduced scaling experimental data over an energy range of below 2 MeV/n. Formula (6.3) scales the experimental data of wider energy range up to X = 2.5 and also describes the cases of non-carbon foils. In /16/ the correction for heavier ions ($Z \geq 54$) has been deduced:

$$\bar{q} = \bar{q}_p [1 - \exp (-12.905 + 0.2124\ Z - 0.00122\ Z^2)] \qquad (6.10)$$

where $\bar{q}_p$ is taken from (6.9).

For the standard deviation Nikolaev and Dmitriev /19/ propose the following expression:

$$\sigma = 0.5 \sqrt{\bar{q}\left[1 - \left(\frac{q}{Z}\right)^{1.67}\right]} \qquad (6.11)$$

The correction for heavier ions (Z≥54) is proposed in /16/:

$$\sigma = \sqrt{\bar{q}_p\,(\,0.07535 + 0.18\,y - 0.2654\,y^2)}, \quad y = \frac{\bar{q}_p}{Z} \qquad (6.12)$$

Some experimental data for the charge distribution of Ar ions behind carbon foils of different thicknesses and energies close to those in the NUCLOTRON booster are presented in Table 3/16/.

The calculated distribution for 5 MeV/n Ar ions and carbon foils is given in Table 4. Formula (6.1) works badly for C and Li ions as for them $\bar{q}$ is too close to Z. The experiments show that the probability for the charge state of C^{6+} ions behind the foil is 94% and for the charge state of Li^{3+} ions it is 99%.

Table 3

Ar^{6+}_{40}, T_n= 5.62 MeV/n

d,μg/cm^2	q				
	14	15	16	17	18
60	1.76	13.69	45.40	32.39	6.74
84	1.26	10.57	39.64	37.86	10.58
120	0.96	8.17	35.11	40.54	14.92
150	0.85	7.95	32.47	42.26	16.78
215	0.55	5.53	26.55	43.79	23.59
300	0.04	3.81	25.10	45.21	25.25

Table 4

Ar^{14+}_{40}. T_n= 5.0 MeV/u
t=100 μg/cm^2

q	14	15	16	17	18
Φ.%	0.5	8.3	36.2	41.4	12.5

7. HEAVY IONS SCATTERING IN THE STRIPPING FOIL

The Coulomb elastic scattering of beam ions in a stripping foil will cause a change of the trajectory slopes.

The mean energy loss of an ion for unit path length when $m_{pr} \leq 0.2\ m_t$, where m_{pr}-the particle mass, m_t-the target nucleus mass is given by [25]:

$$\left[-\frac{dE}{dx}\right]_{el} = \frac{2\pi Z_{pr}^2 Z_t^2 e^4 n m_{pr}}{m_t E_{pr}} \left\{ \ln \sin \frac{\vartheta_{min}}{2} + \frac{1}{2} \frac{m_t^2 - m_{pr} m_t - m_{pr}^2}{(m_{pr} + m_t)^2} \right\} \qquad (7.1)$$

In (7.1) n denotes the number of target atoms in unit volume and E_{pr}- the particle energy.

It can be shown [25] that the ratio of the ionization losses and Coulomb scattering energy losses is:

$$\frac{\left[-\frac{dE}{dx}\right]_{ion}}{\left[-\frac{dE}{dx}\right]_{sct}} = \frac{1}{\left[\frac{m_e Z_t}{A_t m_p}\right]} \approx 4000 \ . \qquad (7.2)$$

where m_p is the proton rest mass and A_t - the atomic weight of the target material.

From (7.2) it follows that the energy losses in Coulomb scattering are negligible.

On the contrary, the particle trajectory changes are very important.

The basic laws of elastic Coulomb scattering have been well-known since the time of the Rutherford's pioneer works.

An important role in accelerator practice is played by the multiple scattering in the foil material.

It can be shown that the multiple scattering mean square angle is [25]:

$$\langle\vartheta^2\rangle = 0.078\ \frac{Z_{pr}^2 Z_t^2 t}{E_{pr}^2 A_t}\ \ln\left\{1.08\cdot 10^2\ \frac{Z_{pr} Z_t^{1/3}}{\beta_{pr}}\sqrt{\frac{t}{A_t}}\right\} \qquad (7.3)$$

where E_{pr} is the particle kinetic energy in MeV and t - the target thickness in g/cm^2.

In [28] the following empirical formula for the multiple scattering mean square angle of heavy ions in solid foils is given:

$$\langle\vartheta^2\rangle = 0.250\ \frac{Z_t(Z_t+1)}{A_t}\ \frac{Z_{pr}^2}{E_{pr}^2}\ t \qquad (7.4)$$

where ϑ is in mrad; stripper thickness t is in μg/cm^2 and particle energy E_{pr} is in MeV.

The average number of scatterings per particle and passage is given by:

$$n_{act} = 0.0392\ \frac{Z_{pr}^2 Z_t^2 \gamma_{pr}^2 t}{A_t E_{pr}^2}\ \frac{1}{\vartheta_\alpha} \qquad (7.5)$$

ϑ_α is the so-called screening angle:

$$\vartheta_\alpha = 4.52\ 10^{-3}\sqrt{1.78\ 10^{-4} Z_{pr}^2 Z_t^{2/3}+\beta_{pr}^2}\ \frac{\sqrt[3]{Z_t}}{E_0 \beta_{pr}^2 \gamma_{pr}} \qquad (7.6)$$

where t is the target thickness in g/cm^2, E_{pr} - the particle

energy in MeV. E_0 - the particle energy in MeV. This gives 92, 91 and 73 scatterings for Ar, C and Li ions respectively i.e. we actually have the case of multiple scattering.

We have calculated the values of Coulomb elastic scattering for several ions of interest for the NUCLOTRON booster.

Those of them which refer to single collisions are given in Table 5 for ϑ_{min} and ϑ_{max}, in Table 6 for the mean square angle and Table 7 for the integral cross sections.

Fig.3 depicts the mean square angle for multiple scattering in the target.

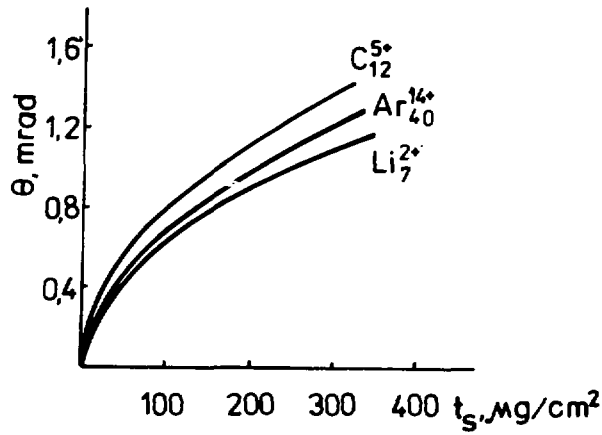

Figure 3. Multiple scattering rms angle for carbon stripping target.

Table 5

ion	Ar_{40}^{14+}	C_{12}^{5+}	Li_7^{2+}
ϑ_{min}	$2.3\ 10^{-6}$	$5.6\ 10^{-6}$	$1.7\ 10^{-5}$
ϑ_{max}	$9.6\ 10^{-3}$	$4.7\ 10^{-2}$	0.12

Table 6

ion	p.20 Mev	Ar_{40}^{14+}	C_{12}^{5+}	Li_{7}^{2+}
$<\theta^2>$	$3.7\ 10^{-3}$	$6.8\ 10^{-11}$	$6.7\ 10^{-10}$	$5.1\ 10^{-9}$

Table 7

ion	p.20 Mev	Ar_{40}^{14+}	C_{12}^{5+}	Li_{7}^{2+}
σ, cm^2	$2.6\ 10^{-18}$	$3\ 7\ 10^{-15}$	$8.8\ 10^{-16}$	$1.4\ 10^{-16}$

8. EMITTANCE GROWTH DUE TO ELASTIC COULOMB SCATTERING IN THE STRIPPING FOIL

It is convenient to work in the normalized phase space (y, y^*), where y is the transverse coordinate (either X or Z) and

$$y^* = \alpha y + \beta y' \qquad (8.1)$$

In (8.1) α and β are the Twiss functions and $'$ denotes differentiation with respect to the longitudinal coordinate S.

In the normalized phase space the betatron oscillations can be presented in the form:

$$y = A \cos(\psi + \alpha)$$
$$y^* = A \sin(\psi + \alpha) \qquad (8.2)$$

where ψ is the betatron phase, $\psi = \int \frac{ds}{\beta(s)}$ and A and α are constants.

Let y and y^* be Gaussian distributions. The betatron amplitude is:

$$A^2 = y^2 + y'^2 \qquad (8.3)$$

Relation (8.3) determines a circle in the normalized phase space with a radius A. In order to find out the amplitude distribution, one has to integrate the joint probability distribution along this circle. In polar coordinates:

$$P(A) = \int_0^{2\pi} p(y,y')A\,d\varphi = \int_0^{2\pi} \frac{A}{2\pi\sigma^2} e^{-\frac{A^2}{2\sigma^2}} d\varphi = \frac{A}{\sigma^2} e^{-\frac{A^2}{2\sigma^2}} \qquad (8.4)$$

i.e. we have obtained Rayleigh distribution with

$$\sigma^2 = 2\sigma_y^2 \qquad (8.5)$$

Passing through the stripper the beam particles change by jump the slope of their trajectory and keep the distance from the equilibrium orbit unchangeable.

$$y = y_0 \ , \ y' = y'_0 + \Delta y' = y'_0 + \beta\Delta y' \qquad (8.6)$$

Behind the stripper we have:

$$A^2 = A_0^2 + 2\Delta y' y'_0 + \Delta y'^2 \qquad (8.7)$$

Averaging (8.7) we obtain:

$$\sigma_A^2 = \sigma_{A0}^2 + \sigma_{\Delta y'}^2 = \sigma_{A0}^2 + \beta_0^2\sigma_{\Delta y'}^2 \qquad (8.8)$$

The real situation in charge exchange injection however is more complicated. At the end of the injection process we have on the accelerator circumference simultaneously particles passing N times through the stripper, particles passing (N-1) times and so on up to the particles having crossed the stripper only once.

Obviously, in this case the probability for an amplitude is

the normalized sum of probabilities for amplitudes after a different number of foil crossings:

$$P(A) = \frac{1}{N} \sum_{i=1}^{N} p_i(A) \tag{8.9}$$

Then

$$\sigma_A^2 = \frac{1}{N} \sum_{i=1}^{N} \sigma_{Ai}^2 \tag{8.10}$$

but

$$\sigma_{Ai}^2 = \sigma_{A0}^2 + \beta_0^2 i \sigma_{\Delta y}^2, \tag{8.11}$$

Thus, we obtain

$$\sigma_A^2 = \sigma_{A0}^2 + \frac{(N+1)}{2} \beta_0^2 \sigma_{\Delta y}^2, \tag{8.12}$$

From (8.12) we can deduce the emittance growth due to elastic Coulomb scattering:

$$\varepsilon_N = \frac{\sigma^2 A}{\beta_0} \cong \varepsilon_0 + \frac{1}{2} N \beta_0 \langle \theta^2 \rangle \tag{8.13}$$

Formula (8.13) differs from a similar formula in /30/ by that we do not restrict ourselves to only one interaction with foil atoms. In fact for low energy heavy ions the integral cross-sections are large enough to have the case of multiple scattering in the target. In (8.13) $\langle \theta^2 \rangle$ is the multiple scattering mean square angle and N denotes the total number of turns.

The calculated emittance growth for the case of the NUCLOTRON booster, is plotted in Fig.4.

9. ENERGY LOSSES IN THE STRIPPING FOIL

The energy losses of beam particles in the stripping foil are mainly due to the excitation and ionization of foil atoms.

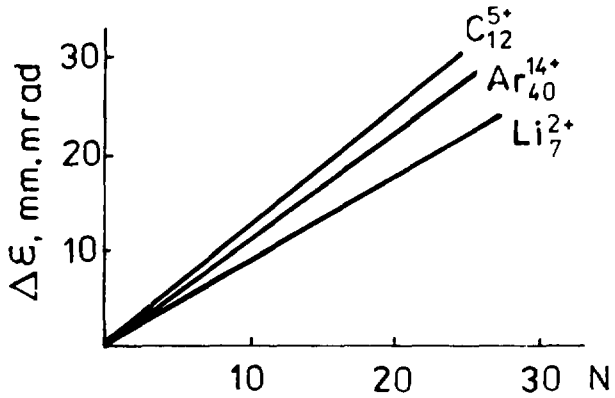

Figure 4. Emittance growth due to multiple scattering: the target thickness 100 $\mu g/cm^2$. $\beta_0 = 4.5$ m.

Mean losses are described by the well-known Bethe-Bloch formula /25-27/:

$$\frac{dE}{dx} = \frac{D\, Z_t \rho_t}{A_t} \left[\frac{Z_{pr}}{\beta}\right]^2 \left(\ln \left(\frac{2\, m_e c^2 \beta^2 \gamma^2}{I} \right) - \beta^2 - \frac{\delta}{2} - \frac{e}{Z_t} \right) (1 + \nu) \qquad (9.1)$$

where ρ is the mass foil density;

$$D = 4\pi N_A r_e m_e e^2 = 0.3070 \ \frac{MeV.cm^2}{g}$$

and I is the mean ionization potential of medium atoms.

$$I = 13.5\, Z_t \ , \ eV \qquad (9.2)$$

δ, c, U are the phenomenological functions which values are usually negligibly small: δ represents the density effect and c - shell corrections.

The energy losses for the test ions are plotted in Fig.5.

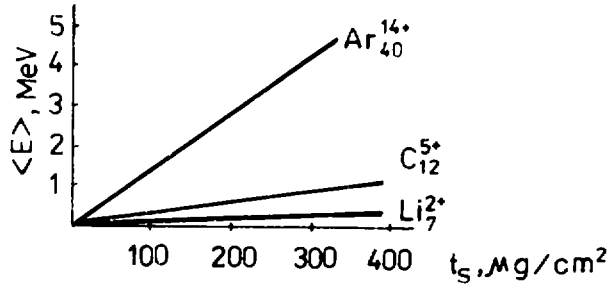

Figure 5. Energy losses in the stripping foil.

10. EMITTANCE GROWTH DUE TO THE ENERGY LOSSES

If the dispersion in the stripper is nonzero then the energy losses will cause the emittance growth according to the well-known relations:

$$\Delta y = - D_0 \frac{\Delta p}{p}$$
$$\Delta y' = - D'_0 \frac{\Delta p}{p} \qquad (10.1)$$

where D_0 and D'_0 are the linear and angular dispersions in the stripper and $\Delta p/p$ is related to the energy losses by:

$$\frac{\Delta E}{E} = \beta^2 \frac{\Delta p}{p} \qquad (10.2)$$

where E is the total particle energy.

The minus sign in (10.1) implies that traversing the foil the particles remain in the same position while due to the energy losses the corresponding off-momentum equilibrium orbit jumps to a new position. We will perform our analysis in the normalized phase space (y, y^*), where betatron oscillations are presented by circles. From a simple geometrical analysis one can deduce that:

$$\sqrt{\beta_0 \varepsilon} = \sqrt{\beta_0 \varepsilon_0} + k \sqrt{\Delta y^2 + \Delta y^{*2}} \qquad (10.3)$$

where, ε_0 is the initial emittance, ε - a new emittance and k- the number of turns.

For the NUCLOTRON booster (10.3) gives quite a large emittance growth. That is why dispersion must be suppressed at the stripper azimuth.

11. IONIZATION LOSSES STRAGGLING IN THE STRIPPING FOIL

The maximum energy transferrable by a fast moving charged particle to the electron is [31]:

$$E_{max} = \frac{2 m_e \beta_{pr}^2 \gamma_{pr}^2 c^2}{1 + 2\gamma \left[\frac{m_e}{m_{pr}}\right] + \left[\frac{m_e}{m_{pr}}\right]^2} \qquad (11.1)$$

For our case $E_{max} = 10.22$ Kev.

The ionization losses are statistical in nature. There exists a probability distribution function $f(x,\Delta)$ so that $f(x,\Delta)d\Delta$ is the probability that the ion, on traversing a path length x in the target, will suffer an energy loss between Δ and $\Delta+d\Delta$.

The character of the distribution function depends on the parameter $\varkappa$ [33]:

$$\varkappa = \frac{\xi}{E_{max}} \qquad (11.2)$$

where

$$\xi = \frac{2\pi n e^4 Z_{pr.eff}^2 Z_t X}{m_e v_{pr}^2} \qquad (11.3)$$

n is the number of target atoms per unit volume, X the target thickness, and $Z_{pr.eff}$ the ion effective charge:

$$Z_{eff} = Z\left[1-\exp\left(-0.95\,\frac{vh}{\alpha^2 Z^{2/3}}\right)\right] \approx Z\left[1-\exp\left(-130\beta Z^{-2/3}\right)\right] \qquad (11.4)$$

a) If $\kappa > 10$ the distribution is highly asymmetric with respect to a Gauss curve, the so called Landau's distribution [32]:

$$f(x,\Delta) = \frac{1}{\xi}\,\varphi(\lambda) \qquad (11.5)$$

$$\varphi(\lambda) = \frac{1}{2\pi i}\int_{c-i\infty}^{c+i\infty} e^{u\ln u + \lambda u}\,du$$

$$\lambda = \frac{\Delta - \xi\left(\ln\frac{\xi}{\varepsilon} + 1 - c\right)}{\xi}$$

where c is Euler's constant c=0.5777... .

$$\ln\varepsilon = \ln\left[\frac{(1-\beta^2)\,I^2}{mv^2}\right] + \beta^2 \qquad (11.6)$$

b) If $0.05 < \kappa < 10$ we have the case of the Vavilov's distribution [33]:

$$f(x,\Delta) = \frac{1}{\pi\xi}\,\kappa\, e^{\kappa(1+\beta^2 c)}\int_0^{\infty} e^{-g(y)}\cos(y f_1 + \kappa f_2)\,dy \qquad (11.7)$$

$$f_1 = \beta^2\left(\ln y - Ci(y)\right) + \cos y + y\,Si(y)$$

$$f_2 = y\left(\ln y - Ci(y)\right) + \sin y + \beta^2 Si(y)$$

where Si and Ci are the sin and cos integral.
c) If $\kappa > 10$ the distribution is Gaussian:

$$f(x,\Delta) = \frac{1}{\sqrt{2\pi\gamma x}}\; e^{-\frac{(\Delta-\alpha x)^2}{2\gamma x}} \qquad (11.8)$$

where according to the Landau's notation.

$$\alpha \equiv \langle \Delta \rangle = \int_0^{\infty} \varepsilon w(\varepsilon)\, d\varepsilon \qquad (11.9)$$

and

$$\gamma = \int_0^{\varepsilon_{max}} \varepsilon^2 w(\varepsilon)\, d\varepsilon = \frac{\xi}{x} \varepsilon_{max} \left(1 - \frac{1}{2} \beta^2 \right) \qquad (11.10)$$

are the mean and variance for unit path length.

The calculated values of χ are: 15 for Ar_{40}^{14+}, 1.9 for C_{12}^{5+} and 0.3 for Li_6^{2+}. This means that the probability distribution is normal for havier ions while it is Vavilov's one for light ions. Thus, the standard deviation for Ar_{40}^{14+} and a 100 mg/cm^2 thickness of the target is $\sqrt{\gamma x}$= 39.1 KeV according to eq.(12.12). The calculated standart deviation is 17 keV for C_{12}^{5+} and 5 keV for Li_6^{2+}.

The Vavilov's distributions for Ca and Li ions are shown in Fig.6 and 7.

The situation with charge exchange injection is a little bit more complicated because we have simultaneously on the orbit particles traversing the foil N-times, (N-1) times up to one time. Then the common probability density is:

$$p(\Delta) = \frac{1}{N} \sum_{i=1}^{N} p_i(\Delta) \qquad (11.11)$$

where $p_i(\Delta)$ is the probability density for particles traversing the foil i-t times.

From (11.11) and taking into account the large value of N, one can deduce for the energy dispersion in a stored beam:

$$\sigma_N^2 = \sigma_0^2 + \frac{N}{2} \sigma_t^2 + \frac{N^2}{12} \langle \Delta \rangle_t^2 \qquad (11.12)$$

where σ_0^2 is the energy dispersion in the incident beam, σ_t^2 is the

dispersion of ionization losses in the foi l material (one passage through the target) and $\langle\Delta\rangle_t$ are mean ionization losses in the foil. The additional momentum spread due to the ionization losses of energy can be calculated from (11.12) and (11.2), see Fig. 8.

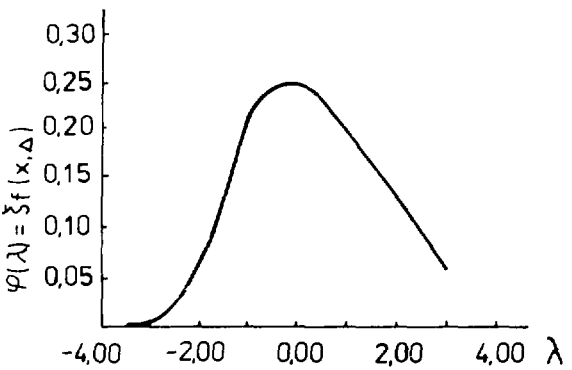

Figure 6. Calculated standart deviation is 17 keV for C_{12}^{5+}

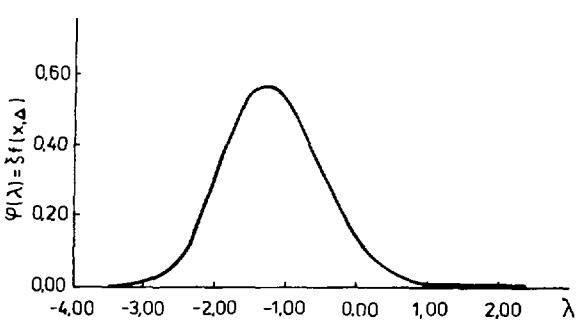

Figure 7. Calculated standart deviation is 5 keV for Li_{12}^{2+}

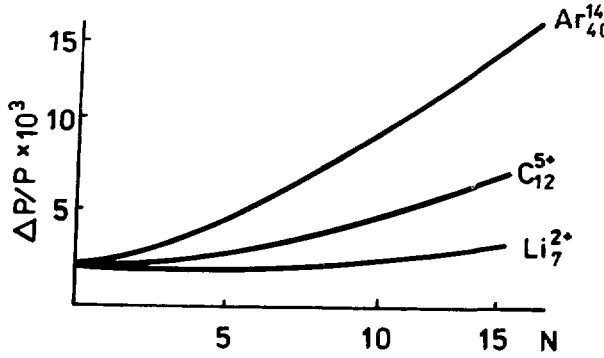

Figure 8. Additional momentum spread due to the ionization losses of energy in the stripping target: the target thickness 100 μg/cm^2

12. ION STORAGE-FIXED ORBIT BUMP MODE

In this mode the orbit bump remains unchangeable. Ions pass through the stripper many times until an equilibrium is attained or until other limited factors - scattering and energy losses begin to restrict the number of stored particles.

The storage process can be described in the following way.

a) During the first turn the number of stored particles will increase as $N_t = \Delta I t$, where $\Delta I = I_0 \sigma_1 n t$ is the ion current behind the target, I_0 the injected beam current, σ_1 the circulating charge ($Z_c \approx \bar{q}$) formation cross section, n the number of target atoms per unit volume, and t the target thickness. At the end of the first turn we will have $N_t = \Delta I.T$ particles on the orbit, T being the period of the synchronous particle..

b) During the second turn the circulating particles will pass through the target for the second time. Let σ_2 be the circulating charge formation cross section for the circulating particles. Generally speaking, $\sigma_2 \neq \sigma_1$ as the charge state distribution in the injected beam differs from that in the circulating beam. If the former is centered on charge number $Z_0 \neq Z_c$ (otherwise charge exchange injection will not work) the circulating beam contains only ions in one charge state. Ions in other charge states have been already lost on the walls of the vacuum chamber because for them $\Delta Z \gg Z_c$ is quite large. Simultaneously new particles are injected into the ring, and these particles will pass through the stripping foil only once. Summarizing, we can obtain for the number of the stored particles:

$$N_t = \Delta I(t-T) + \sigma_2 nt \Delta I(t-T) + \Delta I(2T-t) \qquad (12.1)$$

and at the end of the second turn:

$$N_{2T} = \Delta I(1 + \sigma_2 nt)T \qquad (12.2)$$

Following this way of reasoning, we can obtain for the k-th turn $N_t = \Delta I\,(1 + b + \ldots + b^{k-1})T$, where $b = \sigma_2 nt$. Summing geometrical progression in the brackets, we get:

$$N_k = N_\infty(1-b^k) \qquad (12.3)$$

where

$$N_\infty = \left(\frac{a}{1-b}\right) I_0 T,\ a=\sigma_1 nt,\ b=\sigma_2 nt \qquad (12.4)$$

T is the period of the synchronous particle: I_0 being the injected current, σ_1 the cross section for the formation of ions with equilibrium charge from the injected ions, and σ_2 the cross section for the formation of ions with equilibrium charge from the circulating ions.

In the specific case of stripping target with equilibrium thickness, the charge state distribution behind the target will reach equilibrium which means that it is independent of the charge distribution in the incident beam and that it will be no longer change. For the target of equilibrium thickness $\sigma_1 nt$ =

$\sigma_2 nt = \Phi_{zc}$. i.e. the probability of circulating charge formation for the injected beam is equal to that for the circulating beam. Formula (12.4) becomes simpler:

$$N_k = N_\infty (1 - \Phi_{zc}^k) \tag{12.5}$$

$$N_\infty = \left[\frac{k}{1-\Phi_{zc}}\right] I_0 T \tag{12.6}$$

The curves of the ion storage for the fixed orbit bump mode and the test ions are depicted in Fig. 9.

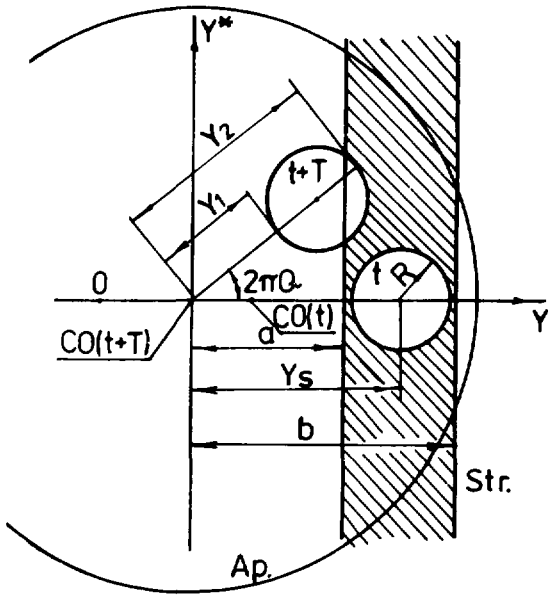

Figure 9. Ion storage for the fixed orbit bump mode.

13. ION STORAGE - MOVING ORBIT BUMP MODE

In this mode the orbit bump gradually reduces to zero during the injection.

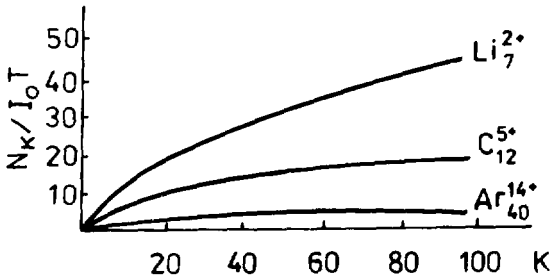

Figure 10. Charge exchange injection with a moving orbit bump.

When the orbit is close to the center of the stripper, the injected particles will cross it every turn. On the contrary the particles injected when the orbit lies outside the stripper will undergo betatron oscillations and will avoid the stripper most of the turns. In other words, we have a kind of combination between the multiturn and the stripping injections. Such a combination allows the number of the injection turns to be increased many times.

The goal of this section is to assess the total number of injected particles in the mode under consideration. We will use a beam model with a uniform charge distribution and clear-cut boundaries wich are circles in the normalized phase space. Let us take a beam slice $dN = I_0 dt$ injected at time t - Fig. 10. After one turn the slice will occupy the position forming angle $\alpha = 2\pi Q$ with the initial position as is depicted in the Fig. 10.

Let us denote by the beam radius by $R = \sqrt{\beta_0 \varepsilon}$ and the

aperture radius by A. As A ≫ R, we will approximate here the aperture boundary lying within the slice confines with a straight line, so the part of the slice outside the aperture will be approximated with a circle segment.

Under the above assumptions a pure geometrical analysis can be carried out. From Fig.8 we obtain that:

$$y_1(t) \approx y_S - R - y_{co}(t)$$
$$y_2(t) \approx y_S + R - y_{co}(t) \qquad (13.1)$$

For the utmost left y' and utmost right y'' projection of the slice on the y axis we have:

$$y'(t+jT) = y_{co}(t+jT) + y_1 \cos j2\pi Q - R\,(1-\cos j2\pi Q)$$
$$y''(t+jT) = y_{co}(t+jT) + y_2 \cos j2\pi Q + R\,(1-\cos j2\pi Q) \qquad (13.2)$$
$$j=0,1,2,....$$

The stripper edge cuts a circle segment with an area S_1 from the beam slice. If H is the edge distance to the slice center we can write:

$$H(t+jT) = a - y_{co}(t+jT) - (y_S - y_{co}(t))\cos j2\pi Q \qquad (13.3)$$

and

$$S_1(t+jT) = R^2 \arccos\left(\frac{H}{R}\right) - H\sqrt{R^2 - H^2}\,, \quad j=0,1,2,.... \qquad (13.4)$$

Another kind of restriction comes from the machine aperture. The aperture is centered on the instantaneous closed orbit position. This means that at the beginning of injection, when the orbit bump passes through the stripper we will have no aperture limitations. However, when the orbit bump is small enough to go close to the machine center considerable aperture restrictions on the beam will take place. The closer the orbit passes to the machine center the stronger aperture restrictions will be.

As mentioned above, we will consider that the aperture cuts also a circle segment (with an area S_c) from the beam slice. This approximation is as much better as A is bigger than R. Similar to (13.4) we can deduce that

$$S_c^2(t)=R\ \arccos\left\{\frac{H_c}{R}\right\} - H_c\sqrt{R^2-H_c^2} \qquad (13.5)$$

where

$$H_c(t)=y_{co}(t) + A - y_s \qquad (13.6)$$

is the distance between the aperture edge and the slice center.

The main parameter of our analysis is the transition coefficient k - the percentage of particles having passed through the stripper and accepted in the aperture.

It can be shown that

$$k(t+jT) = \begin{cases} \Phi, & a<y'(t+jT),\ R<H_c(t) \\ \dfrac{\pi R-S_c(t)}{\pi R^2}\Phi, & a>y'(t+jT),\ H_c(t)<R \\ \dfrac{\pi R^2-(1-\Phi)S_1(t+jT)}{\pi R^2}, & y'(t+jT)<a<y''(t+jT),\ H_c(t)<R \\ \dfrac{\pi R^2-(1-\Phi)S_1(t+jT)-\Phi S_c(t)}{\pi R^2}, & y'(t+jT)<a<y''(t+jT),\ H_c(t)>H(t+jT) \\ \dfrac{\pi R^2-S_c(t)}{\pi R^2}, & y'(t+jT)<a<y''(t+jT),\ H_c(t)<H(t+jT) \\ 1, & y''(t+jT)<a,\ H_c(t)>R \\ \dfrac{\pi R^2-S_c(t)}{\pi R^2}, & y''(t+jT)<a,\ H_c(t)<R \end{cases} \qquad (13.7)$$

$$j=0,1,2\ldots$$

where

$$\Phi = \begin{cases} \sigma_1 nt, & \text{for the injected beam} \\ \sigma_2 nt, & \text{for the circulating beam} \end{cases} \qquad (13.8)$$

is the probability for the formation of ions with equilibrium charge.

.

Let us consider the case of an exponential law of orbit motion:

$$y_{co}(t) = y_S e^{-\frac{t}{\tau}} \tag{13.9}$$

Let r be the number of turns during which the orbit moves from the center of the stripper to the center of the machine.

Let us describe the particle storage turn by turn. During the very first turn:

$$N_1 = \int_0^T \prod_{j=0}^{r} k(t+jT) I_0 dt \tag{13.10}$$

particles will be stored in the ring. Multiplication from 0 to r in (13.10) describes successive crossing of the target while integration describes continuous orbit motion. During the second turn the number of stored particles increases to:

$$N_2 = N_1 + \int_T^{2T} \prod_{j=0}^{r-1} k(t+jT) I_0 dt \tag{13.11}$$

Generating, we arrive at the following expression for the total number of stored particles.

$$N = \sum_{i=0}^{r} \left\{ \int_{iT}^{(i+1)T} \prod_{j=0}^{r-1} k(t+jT) I_0 dT \right\} \tag{13.12}$$

The numerical estimations show that in the present mode of operation the number of the injection turns can be increased more than five times.

14. CONCLUSIONS

The general conclusion from the above analysis is that charge exchange injection could be a powerful method for the injection of light and moderately heavy ions giving a higher intensity than

the other known methods.This is due to the non-Liouville character of the process allowing particles to be injected continuously into one and the same phase space area.

The most important limitation on the stored beam current is due to the ionization losses of energy in the stripping target; the heavier ion the stronger the effect.

In order not to excite betatron oscillations the stripper must be placed at a zero dispersion point.

The additional momentum spread is due to the energy losses in the target and it is produced rather by the different target crossings of the stored particles than by the energy losses straggling.

The additional momentum spread is due to energy losses in the target and it is produced rather by different target crossings of stored particles than by energy losses straggling. Particle scattering causes an emittance growth which is more or less acceptable.

The operation mode with reducing during the injection orbit bump is preferable and in this mode it is possible to increase the circulating beam intensity with respect to the injected beam with a large factor.

REFERENCES

1. G.I.Dimov. *Preprint 304, Institute for Nuclear Physics, Novosibirsk, 1969.*

2. J.D.Simpson. Operating Results from the ANL Booster. *IEEE Trans.on Nucl.Science,NS-20,1973,pp.198-201.*

3. K.Hedblom et al. Calculation on Multiturn and Stripping Injection in CELSIUS. *3-rd EPAC,Berlin,1992.*

4. S.Martin et al. A Storage Ring for the Julich Cyclotron. *Nucl.Instr.and Meth.,A236,1985,pp.249-255.*

5. I.B.Issinsky, V.A.Mikhailov. A 200 Mev/A booster for the LHE

accelerating complex. *Preprint JINR, P1-91-2. 1991, Dubna* (in Russian).

6. D.Dinev. First Turn Simulations in the Cooler Synchrotron COSY. *KFA-Julich,Jul-2499.1991.*

7. F.Ch.Iselin. The MAD Program.(Version 8.4). User's Reference Manual. *CERN/SL/,90-13,(AP),Geneve.1991.*

8. V.S.Nikolaev. Ions interaction effects with matter. *Young scientists school on accelerators charged particles.*

9. I.S.Dmitriev et al. On the target thickness to attain equilibrium charge distribution in a beam of fast ions. *Nucl.Instr.and Meth.,v.B14,1986,pp.515-526.*

10. N.Bohr. *Danske Mat.-Fys.Medd.,v.18.1948,No 8.*

11. N.Bohr, J.Lindhard. *Danske Mat.-Fys.Medd.v.28.1954.No 7.*

12. S.I.Kozlov. About charge exchange cross-sections of heavy ions in gases. *Preprint JINR,9-83-268.Dubna,1983.*

13. B.Franzke. Interaction of stored ion beams with the residual gas. *Forth advanced CERN accelerator school.1992.CERN.92-01.*

14. J.Alouso et al. Charge changing cross sections for heavy ions energies to 8.5 Mev/amu. *IEEE Trans.on Nucl.Sci.,June,1979,pp.1-2.*

15. V.P.Zaikov et.al. Attainment of equilibrium charge distributions in fast ion beams passing through solid films. *Nucl.Instr.and Meth.,v.B5,1984,pp.10-13.*

16. E.Baron, M.Bajard, Ch.Ricaud. Charge exchange of very heavy ions in carbon foils and in the residual gas of GANIL cyclotrons. *Nucl.Instr.and Meth.,v.A328,1993,pp.177-182.*

17. R.B.Clark, I.S.Grant. R.ing, D.A.Eastham, T.Joj. Equilibrium charge state distributions of high energy heavy ions. *Nucl.Instr.and Meth..v.133.1976.pp.17-24.*

18. K.Y.Xuan. R.Droin. Determination semi-empirique des etats de charges d'un faisceau d'ions rapides (Z≤18). *Nucl.Instr.and Meth.v.160.1979.pp.461-463.*

19. V.S.Nikolaev, I.S.Dmitriev. *Phys.Lett.v.28A.1968.p.277.*

20. K.X.To. R.Droin. *Nucl.Instr.and Meth.v.160.1979.p.461.*

21. K.Shima. T.Ishihara, T. Mikumo. Empirical formula for the average equilibrium charge-state of heavy ions behind various foils. *Nucl.Instr.and Meth.v.200.1982.pp.605-608.*

22. H.H.Heckman. E.L.Hubbord. W.G.Simon. *Phys.Rev.v.129.1962. p.1240.*

23. H.D.Betz. G.Horting. I.Leischner. Ch.Schmetzer. B.Steller. J.Weithranch. *Phys.Lett.v.22.1966.p.64.*

24. H.D.Betz. *Rev.Mod.Phys.v.44.1972,p.465.*

25. A.I.Abramov. J.A.Kazanskii. E.C.Matusevich. Experimental Methods of Nuclear Physics. M.,

26. Iu.M.Chirkov. N.P.Iudin. Nuclear Physics. Nauka.M.,1974.

27. K.P.Muchin. Experimental Nuclear Physics. v.1.,M.,1974.

28. T.Joy. Simulation of heavy ion scattering at strippers in beam optics calculations for tandem Van de Graaff accelerators. *Nucl.Instr.and Meth.v.106.1973.pp.237-240.*

29. H.Bruck. Accelerateurs Circulaires de Particules. Presses Universitaires de France,Paris,1966.

30. R.K.Cooper, G.P.Lawrence. Beam Emittance Growth in a Proton Storage Ring Employing Charge Exchange Injection. *IEEE Trans.Nucl.Sci.,v.NS-22,No.3,1975,pp. 1916-1918.*

31. Particle Data Group. *Phys.Lett.,v.170B,No 1,1986.*

32. L.D.Landau. Ionization losses of fast particles. Selected papers,v.1,pp.482-490,M.,1969.

33. P.V.Vavilov. Ionization losses of high energy heavy particles. *JETP,v.32,No.4,pp.920-923,1957.*

Received by Publishing Department
on September 15, 1994.